Journal of Inorganic and General Chemistry
ZAAC
Zeitschrift für anorganische und allgemeine Chemie

DOI: 10.1002/zaac.202100047

ARTICLE

2D-Coordination Polymers Constituted from Indium Halides and Dipyridyl N-Donor Ligands

Thomas C. Schäfer,[a] Jonathan Becker,[a] Alexander E. Sedykh,[a] and Klaus Müller-Buschbaum*[a, b]

Dedicated to Prof. Dr. Christoph Janiak on the Occasion of his 60th Birthday

Four indium-based, 2D coordination polymers (CP) were synthesized utilizing $InCl_3$ and InI_3 and the bidentate ligands 4,4′-bipyridine (bipy), 1,2-di(4-pyridyl)ethylene (bpe) and 1,2-di(4-pyridyl)ethane (bpa). The isoreticular networks $^2_\infty[In_2Cl_6(bipy)]$ (**1**) and $^2_\infty[In_2Cl_6(bpe)]$ (**2**) are constituted by chloride- and ligand-bridged octahedra with a honeycomb like (6,3)-net topology (**hcb** topology). In contrast, $^2_\infty[(In_4Cl_{12})(bpa)_3]$ (**3**) consists of $\{In_4Cl_{12}N_6\}$ units, with each indium atom being coordinated by chloride anions and bpa ligands in an octahedral fashion. Bpa ligands connect indium atoms in two dimensions, forming a semi-regular uninodal 3-c net with the point symbol $(4,8^2)$, as present in the **fes** topology. In $^2_\infty[(InI_3)_2(bpa)_3]$ (**4**), indium is coordinated by three iodide and three bpa ligands in a meridional fashion. In contrast to $^2_\infty[In_2Cl_6(bipy)]$ (**1**) and $^2_\infty[In_2Cl_6(bpe)]$ (**2**), the indium-centered octahedra are linked by the bidentate linker only, but also a honeycomb-like, zigzag-shaped (6,3)-net with a **hcb** topology is formed. The CPs were investigated by SCXRD, PXRD, IR-spectroscopy, and with DTA/TG regarding their thermal properties.

Introduction

Coordination Polymers (CPs)[1–4] and especially Metal-Organic Frameworks (MOFs)[5,6] are a class of materials with a fascinating variety and diversity of solid-state structures,[4] possessing intriguing properties, such as luminescence,[7–9] porosity,[10–12] optical[13] and magnetic[14] properties, as well as catalytic activity[15–17]. This makes the investigation of MOFs and CPs a widely explored field in chemical research in the last two decades.[18–20] The properties of these hybrid materials are the result of a specific combination of inorganic and organic building blocks. However, the synthesis of novel materials including a prediction of their properties is still challenging without knowledge of accessible solid-state structures, including the rather complex structures of CPs and MOFs.[21–25]

To date, only a limited number of examples are known for CPs and MOFs constituted from group 13 metal halides together with N-donor ligands.[26–38] The vast majority is constructed from d-block elements as inorganic building blocks and carboxylates as organic linkers. Group 13 metal trihalides act as strong Lewis acids, forming stable donor acceptor complexes in combination with N-donor ligands.[39] The Lewis acidity and the capability to adopt coordination numbers of four, five and six for the central atom in respective complex compounds makes them to ideal building blocks for the synthesis of CPs and MOFs. Among the group 13 elements and their trivalent ions, In^{3+} seems to be a promising candidate for the synthesis of new coordination polymers with N-donor linkers, since In^{3+} itself is a hard Lewis acid that is yet less explored than its lighter homologues.[40] Only a few examples of CPs have been reported for trivalent indium halides, so far.[34–38] Recently, a couple of coordination polymers based on InX_3 (X=F, Cl, I) and the organic N-donor linkers pyrazine (pyz), 4,4′-bipyridine (bipy) and 2,4,6-tri(4-pyridyl)-1,3,5-triazine (tpt) were reported: $^1_\infty[(InCl_3)_2(pyz)]$,[38] $^1_\infty[InI_3(tpt)]$,[29] $^2_\infty[InF_3(bipy)]$[35–37] and $^3_\infty[(InCl_3)_3(tpt)_2]$.[34] They show the possibility to achieve interlinked structures from the components mentioned.

In this work, we present four indium-based neutral 2D coordination polymers $^2_\infty[In_2Cl_6(bipy)]$ (**1**), $^2_\infty[In_2Cl_6(bpe)]$ (**2**), $^2_\infty[(In_4Cl_{12})(bpa)_3]$ (**3**) and $^2_\infty[(InI_3)_2(bpa)_3]$ (**4**), which were synthesized under solvothermal conditions utilizing the dipyridyle ligands 4,4′-bipyridine (bipy), 1,2-di(4-pyridyl)ethylene (bpe) and 1,2-di(4-pyridyl)ethane (bpa).

[a] *T. C. Schäfer, J. Becker, A. E. Sedykh, Prof. Dr. K. Müller-Buschbaum*
Institute of Inorganic Chemistry
Justus-Liebig Universität Gießen
Heinrich-Buff-Ring 17, 35392 Gießen
E-mail: Klaus.mueller-buschbaum@anorg.chemie.uni-giessen.de
[b] *Prof. Dr. K. Müller-Buschbaum*
Center for Materials Research (LaMa)
Justus-Liebig Universität Gießen
Heinrich-Buff-Ring 16, 35392 Gießen

Supporting information for this article is available on the WWW under https://doi.org/10.1002/zaac.202100047

Results and Discussion

Crystal Structures

The CP $^{2}_{\infty}[In_2Cl_6(bipy)]$ (**1**) crystallizes in the monoclinic crystal system in the space group $P2_1/c$ as colorless crystalline blocks. The coordination polymer is constituted from indium-centered octahedra, in which In^{3+} is axially coordinated by one chlorido ligand and one nitrogen atom of bipy and equatorially by four chlorido ligands. The octahedra are interconnected along the crystallographic *a*-axis to zigzag shaped, edge-connected chains by two chlorido ligands, respectively. In addition, the resulting strands, are linked via N-atoms of bipy ligands forming a two dimensional network. Layers of **1** are stacked along the crystallographic b-axis and shifted along the crystallographic *c*-axis towards each other. A depiction of the crystal structure is given in Figure 1 (see also Figures S1–S2, supporting information).

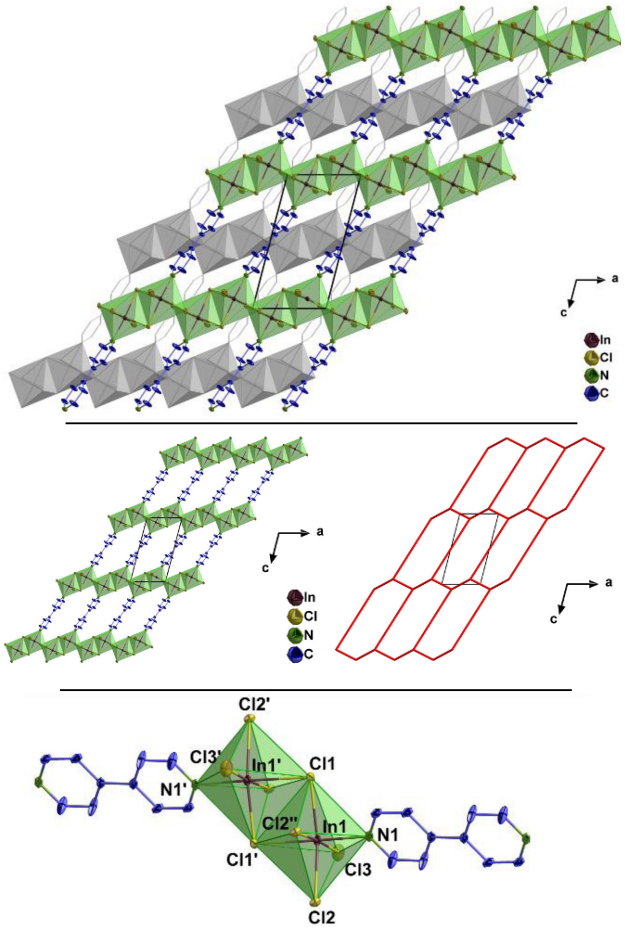

Figure 1. The crystal structure of the 2D coordination polymer $^{2}_{\infty}[In_2Cl_3(bipy)]$ (**1**) (Top) with a view along [0–10]. The polyhedra of the 2D coordination polymer belonging to one 2D-net are highlighted in green, whereas the second layer is marked in grey. Thermal ellipsoids show a 50% probability level of the atoms. For better clarity, all hydrogen-atoms are omitted. One layer of the crystal structure of **1** (Center, left). Topological representation of CP **1** as (6,3)-net or uninodal 3-c net, as present in the **hcb** topology (Center, right). Extended coordination of In^{3+} in **1** (Bottom). Symmetry operations: I = 1−x, 1−y, 1−z, II = 2−x, 1−y, 1−z.

For a better understanding of the otherwise complex crystal structure, also the topology was determined in accordance to the Wells terminology and the three letter code from RCSR.[41–43] In $^{2}_{\infty}[In_2Cl_6(bipy)]$ (**1**), each indium-centered octahedron is regarded as node with a threefold connectivity. Hereby, linkage is achieved via one bipy ligand acting as linker and two chloride double-bridges, edge-connecting the octahedra of **1**. Considering double bridges as bidentate linkage equal to bipy, **1** adopts a 2D (6,3)-net according to the Wells terminology. Thus, the topology of CP **1** can be described as a uninodal 3-c (three-connected) net with the point symbol (6^3), as found in the **hcb** topology (according to RCSR).

The same topology was found for the chemically closely related network $^{2}_{\infty}[In_2Cl_6(bpe)]$ (**2**). However, this applies only to one 2D-net. This means, the connectivity of all nodes as well as the underlying net-topology are the same, although the ligand acting as linker and the packing of the discrete nets differs.[44] A depiction of the crystal structure for CP **2** is given in Figure 2 (see also Figure S3, supporting information).

CP **2** crystallizes in the monoclinic crystal system in the space group $P2_1/c$ as colorless blocks. CP **2** is constituted from indium-centered octahedra, in which In^{3+} is axially coordinated by one chlorido ligand and one nitrogen atom of bpe and equatorially by four chlorido ligands. The linkage of the indium-centered octahedra of CP **2**, forming the 2D CP, is equal to the previously described CP **1**, whereas the individual layers of $^{2}_{\infty}[In_2Cl_6(bpe)]$ are stacking shifted and additionally rotated ($\alpha = 90°$) towards each other along the crystallographic *c*-axis.

$^{2}_{\infty}[(In_4Cl_{12})(bpa)_3]$ (**3**) crystallizes in the triclinic crystal system in the space group $P\bar{1}$. A depiction of the crystal structure is given in Figure 3 (see also Figures S4–S5, supporting information). Like CP **1** and **2**, coordination polymer **3** is constituted from indium atoms being octahedrally coordinated by chlorido- and bpa ligands. In contrast to **1** and **2**, the indium-centered octahedra do not extend to chloride bridged edge-connected chains by two chlorido ligands, respectively. Instead, the structure contains $\{In_4Cl_{12}N_6\}$ units. These units consist of four edge connected octahedra, of which the central double octahedron consists of indium atoms which are coordinated by four chlorido ligands in equatorial positions and, in each case, by one chlorido- and one bpa ligand in axial positions.

The central double octahedron of the $\{In_4Cl_{12}N_6\}$ unit is further edge connected to two terminal In^{3+}-centered octahedra, with the central atom being axially coordinated by two bpa ligands and equatorially by four chlorido ligands. To understand the underlying net-topology, CP **3** is considered as indium-centered octahedra, which are corner-connected by bpa and edge-connected by two chloride bridges, simplifying CP **3** to be a semi-regular uninodal 3-c net, containing two different ring sizes of four and eight. Thus, $^{2}_{\infty}[(In_4Cl_{12})(bpa)_3]$ (**3**) is a two dimensional 3-c net with the point symbol ($4,8^2$) and possesses the **fes** topology.

The 2D coordination polymer $^{2}_{\infty}[(InI_3)_2(bpa)_3]$ (**4**) crystallizes in the monoclinic crystal system in the space group $P2_1/c$ as colorless plates. CP **4** is constituted from slightly distorted, indium-centered octahedra. The meridional coordination is

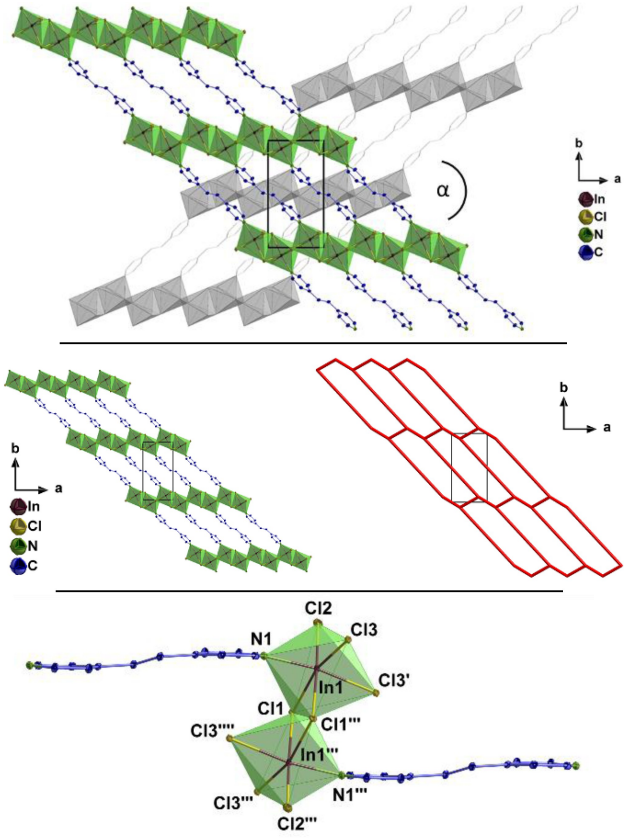

Figure 2. The crystal structure of the 2D coordination polymer $^{2}_{\infty}[In_2Cl_3(bpe)]$ (**2**) with a view along [00–1] (Top). The polyhedra of the 2D coordination polymer belonging to one 2D-net are highlighted in green, whereas the second layer is marked in grey. Thermal ellipsoids show a 50% probability level of the atoms. For better clarity, all hydrogen-atoms are omitted. One layer of the crystal structure of **2** (Center, left). Topological representation of a layer of **2** as (6,3)-net or uninodal 3-c net, as present in the **hcb** topology (Center, right). Extended coordination of In^{3+} in **2** (Bottom). Symmetry operations: I = 2−x, 1−y, 1−z, III = 1-x, 1−y, 1−z, IIII = −1 + x, y, z.

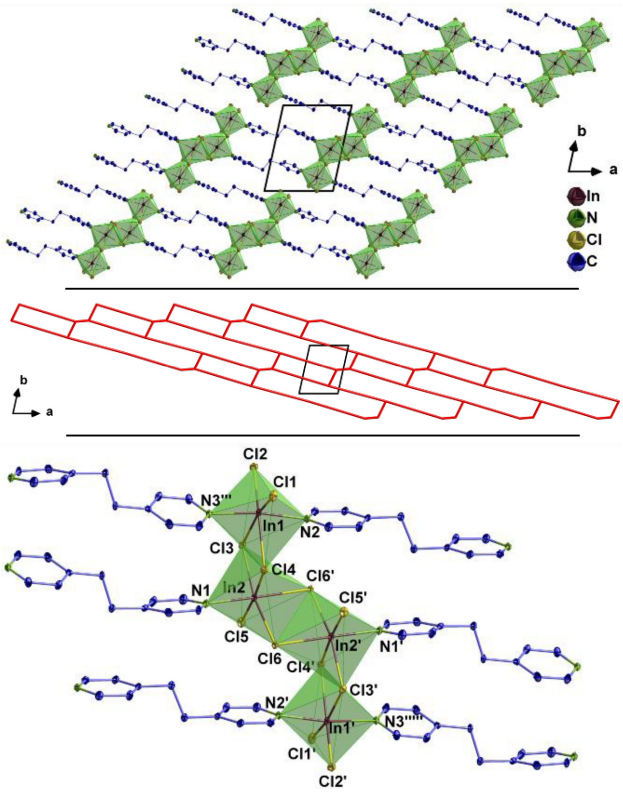

Figure 3. Excerpt of the crystal structure of the 2D coordination polymer $^{2}_{\infty}[(In_4Cl_{12})(bpa)_3]$ (**3**) with a view along [00–1] displaying one layer only (Top). The polyhedra around In^{3+} are highlighted in green. All hydrogen-atoms are omitted and thermal ellipsoids show a 50% probability level of the atoms. Topological representation of **3** as uninodal 3-c net with the point symbol $(4,8^2)$, as present in the **fes** topology (Center). Extended coordination of In^{3+} in **3** (Bottom). Symmetry operations: I = 2−x, 1−y, −z, III = −x, 1−y, 1−z, IIIII = 2 + x, y, −1 + z.

accomplished by three iodido- and three N-donor ligands. Here, only the bpa ligand acts as linker, connecting the octahedra to a 2D network, as depicted in Figure 4 (see also Figure S6–S7, supporting information).

The 2D coordination polymer can be reduced to a (6,3)-net containing six indium-centered nodes with a threefold connectivity for each node. The overall topology for CP **4** is a 2D uninodal 3-c net with the point symbol (6^3), and possesses the **hcb** topology. This topology is identical to **1** and **2**, although no halide bridges are involved in extending the inorganic building blocks. The honeycomb-like structure extends along the crystallographic *b*- and *c*-axis, whereby the discrete zigzag-shaped layers are stacking along the crystallographic *a*-axis.

Due to the relations of the crystal structures, the interatomic In–Cl and In–N distances are in good accordance for CPs **1**–**3**. The interatomic In–N distances deviate only very little and range from 223.3(2) pm to 225.9(2) pm (CP **1**: In–N = 225.2(2) pm; CP **2**: In–N = 223.9(1) pm; CP **3**: In–N = 223.3(2) pm, 223.5(2) pm, 225.9(2) pm) and the interatomic In–Cl are found in the range of 238.6(1) pm–269.6(1) pm. The interatomic In–Cl distances for bridging chlorides are elongated by 10 pm–30 pm compared to the terminal In–Cl distances ($In–Cl_{terminal}$: 239.3(1) pm (CP **1**), 238.57(4) pm (CP **2**) and 240.1(1) pm-242.48(7) pm (CP **3**)), as expected. The largest interatomic In–Cl distance was found to be 269.6(1) pm for a bridging chloride in **3** (In1-Cl3). A comparison of these values can be drawn to the ladder-like, double stranded one-dimensional coordination polymer $^{1}_{\infty}[(InCl_3)_2(pyz)_3]$,[38] which consists of pyrazine linked In^{3+}-centered octahedra. It shows interatomic distances of 232.7 pm, 237.2 pm (In–N) and 239.7 pm, 241.7 pm (In–Cl) matching for the interatomic In–Cl distances to terminal chloride ions, whereas the interatomic In–N distances of CP **1**–**3** are 10 pm shorter with respect to $^{1}_{\infty}[(InCl_3)_2(pyz)_3]$.

The interatomic distances in coordination polymer $^{2}_{\infty}[(In-I_3)_2(bpa)_3]$ (**4**) for In–I were determined to be 279.8(1) pm, 284.1(1) pm, 287.1(1) pm and 233.8(2) pm, 234.4(2) pm, 235.5(2) pm for In–N, which is also in an expected range. A comparison with the structurally related complex $[InI_3(py)_3]$ (py =

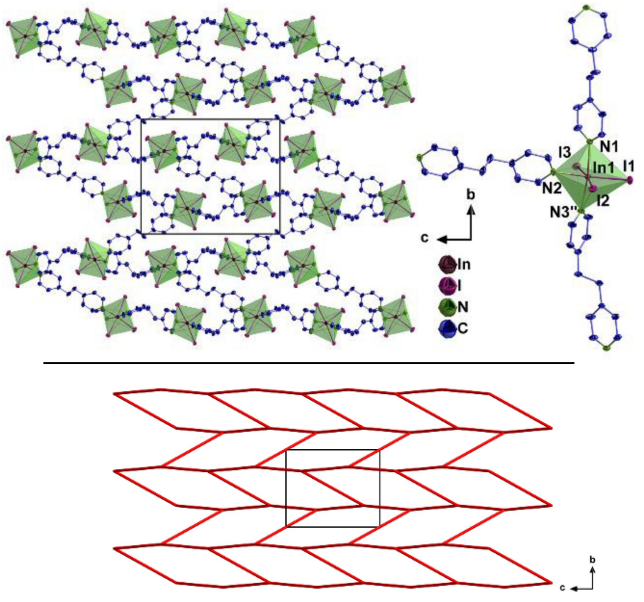

Figure 4. The crystal structure of the 2D coordination polymer $^{2}_{\infty}$ [$(InI_3)_2(bpa)_3$] (**4**) with a view along [−100] (Top, left). The polyhedra around In^{3+} are highlighted in green. For better clarity, all hydrogen-atoms are omitted and thermal ellipsoids show a 50% probability level of the atoms. Extended coordination of In^{3+} in **4** (Top, right). Symmetry operations: II = −1 + x, 1.5 − y, 0.5 + z. Topological representation of **4** as (6,3)-net or uninodal 3-c net with **hcb** topology (Bottom).

pyridine),[45] which also exhibits an octahedral coordination of In^{3+} and interatomic distances of 283.9 pm–286.7 pm (In–I) and 230.9 pm–232.3 pm (In–N), indicates good agreement with **4**. The one-dimensional coordination polymer $^{1}_{\infty}$[InI_3(tpt)] (tpt = 2,4,6-tri(4-pyridyl)-1,3,5-triazine), which consists of trigonal bipyramidally coordinated In^{3+}, shows interatomic distances for In–I = 270.2 pm–270.3 pm and In–N = 241.2 pm). The longer In–I distances found for CP **4** can be explained by the increase in coordination number from five to six.[29]

Altogether, the chlorine containing coordination polymers $^{2}_{\infty}$[In_2Cl_6(bipy)] (**1**), $^{2}_{\infty}$[In_2Cl_6(bpe)] (**2**) and $^{2}_{\infty}$[$(In_4Cl_{12})(bpa)_3$] (**3**) are structurally closely related, whereas the iodine containing $^{2}_{\infty}$[$(InI_3)_2(bpa)_3$] (**4**) shows differences especially in the interlinkage.

Synthesis, IR Spectroscopy and Thermal Analysis

The herein described coordination polymers were achieved in reactions of the indium halides $InCl_3$ and InI_3 with the bidentate N-donor ligands 4,4′-bipyridine, 1,2-di(4-pyridyl)ethylene and 1,2-di(4-pyridyl)ethane. Altogether, four CPs were successfully characterized: $^{2}_{\infty}$[In_2Cl_6(bipy)] (**1**), $^{2}_{\infty}$[In_2Cl_6(bpe)] (**2**), $^{2}_{\infty}$[$(In_4Cl_{12})(bpa)_3$] (**3**) and $^{2}_{\infty}$[$(InI_3)_2(bpa)_3$] (**4**). Summarizing, **1**, **2** and **4** were synthesized as bulk, containing small amounts of unknown complex side phases constituted from the employed precursors, whereas **3** forms as side product.

Stoichiometric reactions of $InCl_3$ or InI_3 with the respective linker in m-xylene using solvothermal conditions and applying temperatures of 185 °C under stirring lead to bulk materials containing **1**, **2** and **4** as main phases. This procedure does not result in an adequate bulk of CP **3**, as shown by PXRD analysis. For depictions of the diffraction patterns of **1**–**3**, see supporting information, Figures S8–S10.

The diffraction patterns of CP **1**, **2** and **4** comply well in terms of reflection positions and intensities with the respective simulated powder diffractogram from single crystal data, although additional reflections of crystalline side phases are observed (see Figure 5 for **4**: 10.8°, 14.6° in 2θ, as well as Figures S8–S10, SI). In all cases, the observed additional reflections do neither originate from the employed indium halides, nor from the crystalline ligands.[46–48] The latter is reasonable due to the extensive washing procedure, which is carried out to remove soluble phases such as the ligands. The finding is also confirmed by IR-spectroscopy, showing no typical vibration modes of the free ligands, but of coordinated, only (see also Figures S11–S17, supporting information). Especially, the ν(C=N) ring vibration modes of the ligands are hypsochromically shifted in all bulk materials (CP **1**: ν(C=N) = 1611 cm^{-1}; CP **2**: ν(C=N) = 1611 cm^{-1}; CP **3**: ν(C=N) = 1615 cm^{-1}; CP **4**: ν(C=N) = 1610 cm^{-1}), indicating coordination to $InCl_3$ or InI_3. Furthermore, the ν(C=N) ring vibration modes for the uncoordinated N-donor ligands (bipy: ν(C=N) = 1587 cm^{-1}; bpe: ν(C=N) = 1594 cm^{-1}; bpa: ν(C=N) = 1593 cm^{-1}) were not observed.[29]

The experimental powder diffractogram of **3** indicates the successful formation of CP **3**. Additional reflections, which could be assigned to $InCl_3$ and at least one unknown, further crystalline phase are observed. Thus, CP **3** is only formed as side phase in the herein described synthetic procedure. Since IR-analysis confirms the absence of free bpa in **3**, the bulk material may contain further product compounds, constituted from the used precursors. This may also hint to further possible products of the reactions leading to **1**, **2** and **4**, although in lower

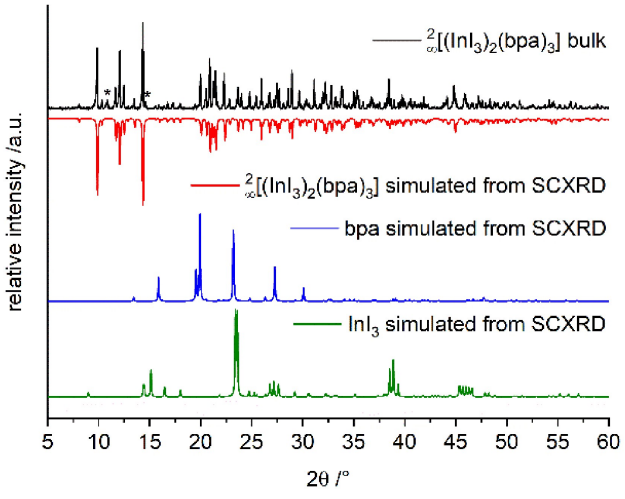

Figure 5. Comparison of the experimental (black) and simulated (red) diffraction patterns of CP **4**, bpa (blue) and InI_3 (green). Reflections of crystalline phases apart from the product coordination polymer are marked with asterisks. (Cu–$K_{\alpha 1}$ = 154.1 pm)

amounts than for **3**. Because of the poor phase purity, no additional bulk analyses were carried out for **3**.

According to elemental analysis of **1**, the CHN-values are slightly increased compared to expected values (Elemental analysis for **1**: Calculated: C = 20.07 %, H = 1.35 %, N = 4.68 %; Found: C = 21.97 %%, H = 1.51 %, N = 4.92 %), which also hints at the formation of low amounts of another phase. In contrast, the elemental analysis of **4** reveals lower CHN-values as calculated (Elemental analysis for **4**: Calculated: C = 28.01 %, H = 2.35 %, N = 5.44 %; Found: C: 26.80 %%, H: 2.12 %, N: 4.96 %), pointing at a more In–I-rich side phase compared to **4**.

Simultaneous DTA/TG investigations of $^{2}_{\infty}$[In_2Cl_6(bipy)] (**1**), $^{2}_{\infty}$[In_2Cl_6(bpe)] (**2**) and $^{2}_{\infty}$[$(InI_3)_2$(bpa)$_3$] (**4**) were carried out to determine the thermal properties (see also Figures S18–S20, supporting information). The chemically and structurally closely related coordination polymers **1** and **2** show strongly related results in the heat flow. Both possess initial, endothermic phase transitions correlating with no detectable mass loss in the TG-curve at onset temperatures of 375 °C (CP **1**) and 330 °C (CP **2**), which are not yet resolved. For **2**, the onset temperature of 330 °C depicts the beginning of two overlapping endothermic processes. Upon further heating, formed intermediate phases decompose with an initial mass loss at onset temperatures of 430 °C (CP **1**) and 400 °C (CP **2**). The thermally least stable coordination polymer $^{2}_{\infty}$[$(InI_3)_2$(bpa)$_3$] (**4**) shows endothermic decomposition with an onset temperature of 250 °C, whereby the correlating DTA-signal depicts the beginning of four consecutive endothermic processes correlating with a complex mass loss. The overall remaining residual mass for all is remarkably low (lowest for **4**: 7 %), with no distinct products that can be identified.

Conclusions

Four 2D coordination polymers originating from the indium halides $InCl_3$ and InI_3 and the bidentate dipyridyl ligands 4,4′-bipyridine (bipy), 1,2-di(4-pyridyl)ethylene (bpe) and 1,2-di(4-pyridyl)ethane (bpa) were synthesized. The resulting compounds $^{2}_{\infty}$[In_2Cl_6(bipy)] (**1**), $^{2}_{\infty}$[In_2Cl_6(bpe)] (**2**), $^{2}_{\infty}$[(In_4Cl_{12})(bpe)$_3$] (**3**) and $^{2}_{\infty}$[$(InI_3)_2$(bpa)$_3$] (**4**) enlarge the limited number of coordination polymers known for indium together with N-donor ligands. They were obtained as single crystals for all compounds and as bulk materials for **1**, **2**, **4** via solvothermal reactions in toluene and m-xylene. In all structures, indium is octahedrally coordinated by halide anions and N-atoms of the dipyridyl ligands. Two CPs (**1** and **2**) exhibit a honeycomb like (6,3)-net **hcb** topology with different packing of the 2D nets, whereas $^{2}_{\infty}$[In_2Cl_6(bpa)] (**3**) adopts **fes** topology with a semi-regular uninodal 3-c net with the point symbol (4,8^2). Structurally related but different from **1**–**3**, $^{2}_{\infty}$[$(InI_3)_2$(bpa)$_3$] (**4**) exhibits a uninodal 3-c net, resulting in a honeycomb-like, zigzag-shaped (6,3)-net, also of **hcb** topology. Furthermore, thermal investigations were carried out for CP **1**, **2** and **4** revealing a stability of the phases up to temperatures of 375 °C (CP **1**), 330 °C (CP **2**) and 250 °C (CP **4**).

Experimental Section

Because of the air and moisture sensitivity of the group 13 metal halides and the obtained reaction products, all reactions and manipulations were carried out under inert gas atmosphere in Duran® glass ampoules, using vacuum line, Schlenk and glovebox (MBraun, Labmaster SP, and Innovative Technology, Pure Lab) techniques. The reactions in Duran® glass ampoules were performed in a Büchi glass-furnace as well as in heating furnaces based on Al_2O_3 tubes with Kanthal wire resistance and NiCr/Ni temperature elements. The heating programs were applied using Eurotherm 2416 control units. The starting materials $InCl_3$ (anhydrous, 99.999 %, Sigma-Aldrich) and InI_3 (anhydrous, 99.998 %, Sigma-Aldrich) were used as purchased. 1,2-Di-(4-pyridyl)ethylene (97 %, Sigma-Aldrich), 1,2-Di-(4-pyridyl)ethane and 4,4′-Bipyridine was purified by sublimation prior to reactions. Toluene was dried by distillation under dry argon atmosphere from sodium and stored over activated molecular sieves (4 Å). m-Xylene (99 %, extra dry, Acros Organics) was degassed and stored over activated molecular sieves (4 Å) for 3 days prior to use.

Microanalyses were carried out on a Thermo FlashEA-1112 series analyser. IR-spectra were recorded with a Bruker VERTEX70/Platinum spectrometer in transmission mode using an ATR-unit. Thermal properties were determined by simultaneous DTA/TG (NETZSCH STA 409-PC) in a constant argon flow of 50 ml·min^{-1} with a heating rate of 5 K·min^{-1} from room temperature to 1000 °C.

X-ray crystallography. Single crystal X-ray determinations of $^{2}_{\infty}$[In_2Cl_6(bipy)] (**1**), $^{2}_{\infty}$[In_2Cl_6(bpe)] (**2**), $^{2}_{\infty}$[(In_4Cl_{12})(bpa)$_3$] (**3**) and $^{2}_{\infty}$[$(InI_3)_2$(bpa)$_3$] (**4**) were performed on a BRUKER AXS Smart Apex 1 diffractometer with graphite monochromator (MoK_α radiation; λ = 0.71073 Å). Data collections for the compounds **1**, **2**, **3** were performed at 100 K, whereas data collection for compound **4** was performed at 200 K due to cracking of crystal upon further cooling. The structures were solved using direct methods, refined with the least-squares method as implemented in ShelXL[49,50] and expanded using Fourier techniques, all within the OLEX2 software suite.[51] All non-hydrogen atoms were refined anisotropically. Hydrogen atoms were assigned to idealized geometric positions and included into structure factors calculations. Depictions of the crystal structures were created using DIAMOND.[52] Topological determinations were carried out using the ToposPro program package.[53] The crystallographic data has been deposited at the Cambridge Crystallographic Data Centre as CCDC 2061039 (CP **1**), 2061040 (CP **2**), 2061041 (CP **3**), 2061042 (CP **4**).

Crystal data for **1**, ($C_5H_4Cl_3InN$) (M = 299.26 g·mol^{-1}): monoclinic, space group $P2_1/c$ (no. 14), a = 622.6(4) pm, b = 1262.9(8) pm, c = 1172.7(8) pm, β = 104.51(1)°, Z = 4, T = 100.0 K, μ(MoK_α) = 3.470 mm^{-1}, ρ_{calc} = 2.227 g·cm^{-3}, 66731 reflections observed (6.452° ≤ 2θ ≤ 72.356°), 4245 unique (R_{int} = 0.0575, R_{sigma} = 0.0242), which were used in all calculations. Final R_1 = 0.0192 ($I > 2\sigma(I)$) and ωR_2 = 0.0382 (all data).

Crystal data for **2**, ($C_6H_5Cl_3InN$) (M = 312.28 g·mol^{-1}): monoclinic, space group $P2_1/c$ (no. 14), a = 613.03(4) pm, b = 1178.48(8) pm, c = 1219.21(8) pm, β = 91.397(1)°, Z = 4, T = 100.15 K, μ(MoK_α) = 3.523 mm^{-1}, ρ_{calc} = 2.356 g·cm^{-3}, 22689 reflections observed (6.648° ≤ 2θ ≤ 61.198°), 2703 unique (R_{int} = 0.0238, R_{sigma} = 0.0117), which were used in all calculations. Final R_1 = 0.0127 ($I > 2\sigma(I)$) and ωR_2 = 0.0294 (all data).

Crystal data for **3**, ($C_{18}H_{18}Cl_6In_2N_3$) (M = 718.69 g·mol^{-1}): triclinic, space group P-1 (no. 2), a = 915.3(1) pm, b = 1223.5(2) pm, c = 1262.3(2) pm, α = 63.873(4)°, β = 69.407(4)°, γ = 70.435(4)°, Z = 2, T = 100 K, μ(MoK_α) = 2.689 mm^{-1}, ρ_{calc} = 2.057 g·cm^{-3}, 52042 reflections observed (5.358° ≤ 2θ ≤ 57.04°), 5820 unique (R_{int} = 0.0736,

R_{sigma} = 0.0397), which were used in all calculations. Final R_1 = 0.0262 ($I > 2\sigma(I)$) and wR_2 = 0.0605 (all data).

Crystal data for **4**, ($C_{18}H_{18}I_3InN_3$) (M = 771.87 g·mol^{-1}): monoclinic, space group $P2_1/c$ (no. 14), a = 909.36(7) pm, b = 14.12.5(1) pm, c = 1742.3(1) pm, β = 100.922(1)°, Z = 4, T = 200.0 K, μ(MoKα) = 5.297 mm^{-1}, ρ_{calc} = 2.333 g·cm^{-3}, 63904 reflections observed (5.398° ≤ 2 θ ≤ 66.478°), 8428 unique (R_{int} = 0.0545, R_{sigma} = 0.0292), which were used in all calculations. Final R_1 = 0.0262 ($I > 2\sigma(I)$) and wR_2 = 0.0629 (all data).

PXRD analysis. Powder X-ray diffraction was carried out on a STOE STADI P diffractometer with focusing Ge(111) monochromator and a Dectris MYTHEN 1 K strip detector in Debye-Scherrer geometry. Powder samples were prepared in Lindemann glass capillaries with 0.5 mm diameter (for **1**–**3**, bipy, bpe and bpa) and due to high absorption in capillaries with 0.2 mm diameter (for **4** and $InCl_3$, InI_3) under inert gas atmosphere. The samples were measured in transmission geometry using CuK_α radiation (λ = 1.54056 Å).

General Synthesis and Safety Procedure. The herein described procedures contain working steps, in which hot ampoules with gas-overpressure were handled outside heating furnaces, provoking safety issues. Therefore, appropriate safety precautions, such as Kevlar® gloves, face protection and splinter shield have to be considered. It should further be stated, that any further instrumentation was annealed to the respective oven temperatures before touching hot ampoules. The herein reported single crystal and bulk syntheses for $^2_\infty$[In_2Cl_6(bipy)] (**1**), $^2_\infty$[In_2Cl_6(bpe)] (**2**), $^2_\infty$[(In_4Cl_{12})(bpa)$_3$] (**3**) and $^2_\infty$[(InI_3)$_2$(bpa)$_3$] (**4**) were carried out in Duran® glass ampoules under solvothermal conditions.

Procedure one. For syntheses of single crystals, different conditions were applied compared to bulk syntheses. In general, for single crystals of suitable size and quality for a structure determination, the reagents were mixed in a mortar and sealed in an ampoule under reduced pressure. Solvents were frozen using liquid nitrogen before applying vacuum (p = 1.0·10^{-3} mbar) to the ampoule as well as for sealing of the ampoule. Subsequently, the ampoules were placed in a tubular furnace, and a heating program with three steps was applied. In the first step, the reaction mixture was heated to a temperature of 190 °C (**3**) or 195 °C (**1**, **2** and **4**) within 1 h. The respective temperature was kept in step two for 384 h (**3**) or 672 h (**1**, **2** and **4**) before the oven was finally cooled to room temperature within 24 h (**1**–**4**).

Procedure two. The bulk syntheses of **1**–**4** were carried out in ampoules under solvothermal conditions utilizing 1 ml m-xylene as solvent. The solvent was frozen using liquid nitrogen before applying vacuum (p = 1.0·10^{-3} mbar) to the ampoules as well as before sealing of the ampoules. The solid reagents were mixed in a mortar and sealed together with a stirring bar in the ampoule. Afterwards, the prepared reaction mixtures were treated in an ultrasonic bath for 30 min and subsequently stirred at room temperature for 1 h. In the next step, the ampoules were placed in a Büchi glass furnace equipped with a magnetic stirrer. The reaction mixtures were heated to 185 °C within 2 h under stirring. After 2 h at 185 °C, the hot ampoules were taken out of the oven, cooled to room temperature and treated in an ultrasonic bath for 30 min. Then, the ampoules were placed again in a pre-heated Büchi glass furnace and stirred at 185 °C for 16 h. Subsequently, the hot ampoules were removed from the oven, cooled to room temperature and centrifuged for 10 min at 4000 rpm, allowing the solid reaction products to settle down at the bottom of the ampoule. Again, the ampoules were placed in the hot Büchi glass furnace, and kept without stirring for another hour at 185 °C. Afterwards, the solvent was removed from the solid reaction product by decanting. This step was accomplished by fast and careful turning of the hot ampoule outside the oven. Then, the reaction products were cooled to room temperature and washed three times with 1 ml boiling toluene and finally dried at dynamic vacuum (p = 1.0·10^{-3} mbar) at room temperature.

Synthesis of $^2_\infty$[In_2Cl_6(bipy)] (**1**) was achieved according to general procedure two by reaction of 111 mg (1 eq., 502 μmol) $InCl_3$ with 40 mg (0.5 eq., 256 μmol) bipy. This procedure leads to a colorless bulk material with **1** as main phase. The obtained product was characterised by PXRD-analysis, IR-spectroscopy as well as CHN-analysis. Yield: 132 mg (87 %, referred to initial mass of reactants). The colorless product is air and moisture sensitive. Elemental analysis calculated for $C_{10}H_8Cl_6In_2N_2$: C: 20.07 %, H: 1.35 %, N: 4.68 %. Found: C: 21.97 %, H: 1.51 %, N: 4.92 %. FTIR (ATR): $\tilde{\nu}$ = 3231 (w), 3180 (w), 3088 (w), 1611 (s), 1536 (w), 1493 (m), 1416 (s), 1366 (w), 1221 (m), 1068 (s), 1015 (m), 851 (w), 807 (s), 763 (s), 722 (m), 641 (s), 563 (m), 482 (m) cm^{-1}.

Single crystal synthesis of $^2_\infty$[In_2Cl_6(bipy)] (**1**) was accomplished according to general procedure one by solvothermal reaction of 111 mg (1 eq., 502 μmol) $InCl_3$ with 40 mg (0.5 eq., 256 μmol) bipy in 0.5 ml toluene. This procedure leads to a reaction mixture with colorless single crystals of **1**.

Synthesis of $^2_\infty$[In_2Cl_6(bpe)] (**2**) was achieved according to general procedure two by reaction of 111 mg (1 eq., 502 μmol) $InCl_3$ with 46 mg (0.5 eq., 252 μmol) bpe. This procedure leads to a colorless bulk material with **2** as main phase. The obtained product was characterised by PXRD-analysis, IR-spectroscopy as well as CHN-analysis. Yield: 100 mg (64 %, referred to initial mass of reactants). The colorless product is air and moisture sensitive. Elemental analysis calculated for $C_{12}H_{10}Cl_6In_2N_2$: C: 23.08 %, H: 1.61 %, N: 4.49 %. Found: C: 23.77 %, H: 1.71 %, N: 4.36 %. FTIR (ATR): $\tilde{\nu}$ = 3086 (w), 1629 (m), 1611 (s), 1504 (w), 1432 (m), 1351 (w), 1298 (w), 1225 (w), 1207 (m), 1067 (m), 1024 (s), 965 (m), 826 (s), 791 (m), 761 (m), 729 (w), 569 (s), 546 (m), 476 (m) cm^{-1}.

Single crystal synthesis of $^2_\infty$ In_2Cl_6(bpe)] (**2**) was achieved according to general procedure one by solvothermal reaction of 111 mg (1 eq., 502 μmol) $InCl_3$ with 46 mg (0.5 eq., 252 μmol) bpe in 0.5 ml toluene. This procedure leads to a reaction mixture with colorless single crystals of **2**.

Synthesis of $^2_\infty$[(In_4Cl_{12})(bpa)$_3$] (**3**) was carried out according to general procedure two by reaction of 111 mg (4 eq., 502 μmol) $InCl_3$ with 69 mg (3 eq., 375 μmol) bpa. This procedure leads to a colorless bulk material with **3** as minor phase. The obtained product was characterised by PXRD-analysis and IR-spectroscopy. Yield: 133 mg (74 %, referred to initial mass of reactants). The colorless mixture is air and moisture sensitive. FTIR (ATR): $\tilde{\nu}$ = 2935 (w), 1615 (s), 1561 (w), 1504 (w), 1453 (w), 1433 (s), 1226 (m), 1211 (w), 1069 (m), 1025 (s), 882 (w), 831 (s), 818 (m), 785 (w), 832 (w), 543 (s), 489 (m) cm^{-1}.

Single crystal synthesis of $^2_\infty$[(In_4Cl_{12})(bpa)$_3$] (**3**) was carried out according to general procedure one by solvothermal reaction of 111 mg (1 eq., 502 μmol) $InCl_3$ with 92 mg (1 eq., 499 μmol) bpa in 0.5 ml toluene. This procedure leads to a reaction mixture containing colorless single crystals of **3**.

Synthesis of $^2_\infty$[(InI_3)$_2$(bpa)$_3$] (**4**) was accomplished according to general procedure two by reaction of 124 mg (2 eq., 249 μmol) InI_3 with 69 mg (3 eq., 252 μmol) bpa. This procedure leads to a colorless bulk material with **4** as main phase. The obtained product was characterised by PXRD-analysis, IR-spectroscopy as well as CHN-analysis. Yield: 133 mg (69 %, referred to initial mass of reactants). The colorless product is air and moisture sensitive. Elemental analysis calculated for $C_{36}H_{36}I_6In_2N_6$: C: 28.01 %, H: 2.35 %, N: 5.44 %. Found: C: 26.80 %, H: 2.12 %, N: 4.96 %. FTIR (ATR): $\tilde{\nu}$ = 2927 (w), 1610 (s), 1557 (w), 1502 (w), 1449 (w), 1427 (s), 1224 (m),

1212 (m), 1063 (m), 1012 (s), 873 (w), 821 (s), 811 (s), 627 (w), 544 (s), 534 (s), 490 (s) cm^{-1}.

Single crystal synthesis of $^{2}_{\infty}[(InI_3)_2(bpa)_3]$ (**4**) was achieved according to general procedure one by solvothermal reaction of 99 mg (1 eq., 200 µmol) InI_3 with 37 mg (1 eq., 201 µmol) bpa in 0.5 ml toluene. This procedure leads to a reaction mixture with colorless single crystals of **4**.

Acknowledgements

The authors gratefully acknowledge support of the Deutsche Forschungsgemeinschaft within SPP1928 "COORNETs" for the project MU-1562/13-1. A. E. Sedykh gratefully acknowledges the Studienstiftung des Deutschen Volkes for a PhD fellowship. Open access funding enabled and organized by Projekt DEAL.

Keywords: Coordination polymers · Indium · 4,4'-bipyridine · 1,2-di(4-pyridyl)ethylene · 1,2-di(4-pyridyl)ethane

[1] C. Janiak, *Dalton Trans.* **2003**, 2781–2804.
[2] H. Furukawa, K. E. Cordova, M. O'Keeffe, O. M. Yaghi, *Science* **2013**, *341*, 1230444.
[3] C. Janiak, J. K. Vieth, *New J. Chem.* **2010**, *34*, 2366.
[4] S. Kitagawa, R. Matsuda, *Coord. Chem. Rev.* **2007**, *251*, 2490–2509.
[5] S. R. Batten, N. R. Champness, X.-M. Chen, J. Garcia-Martinez, S. Kitagawa, L. Öhrström, M. O'Keeffe, M. Paik Suh, J. Reedijk, *Pure Appl. Chem.* **2013**, *85*, 1715–1724.
[6] S. Bauer, N. Stock, *Chem. Unserer Zeit* **2008**, *42*, 12–19.
[7] J. R. Sorg, T. C. Schäfer, T. Schneider, K. Müller-Buschbaum, *Z. Anorg. Allg. Chem.* **2020**, *646*, 507–513.
[8] J. Heine, K. Müller-Buschbaum, *Chem. Soc. Rev.* **2013**, *42*, 9232–9242.
[9] L. V. Meyer, F. Schönfeld, K. Müller-Buschbaum, *Chem. Commun.* **2014**, *50*, 8093–8108.
[10] N. A. Khan, Z. Hasan, S. H. Jhung, *J. Hazard. Mater.* **2013**, *244–245*, 444–456.
[11] X. Zhang, Z. Chen, X. Liu, S. L. Hanna, X. Wang, R. Taheri-Ledari, A. Maleki, P. Li, O. K. Farha, *Chem. Soc. Rev.* **2020**, *49*, 7406–7427.
[12] S. Kitagawa, R. Kitaura, S.-i. Noro, *Angew. Chem. Int. Ed.* **2004**, *43*, 2334–2375; *Angew. Chem.* **2004**, *116*, 2388–2430.
[13] R. Medishetty, J. K. Zaręba, D. Mayer, M. Samoć, R. A. Fischer, *Chem. Soc. Rev.* **2017**, *46*, 4976–5004.
[14] G. Mínguez Espallargas, E. Coronado, *Chem. Soc. Rev.* **2018**, *47*, 533–557.
[15] M. Y. Masoomi, A. Morsali, A. Dhakshinamoorthy, H. Garcia, *Angew. Chem. Int. Ed.* **2019**, *58*, 15188–15205.
[16] A. Corma, H. García, F. X. Llabrés i Xamena, *Chem. Rev.* **2010**, *110*, 4606–4655.
[17] J. Liu, L. Chen, H. Cui, J. Zhang, L. Zhang, C.-Y. Su, *Chem. Soc. Rev.* **2014**, *43*, 6011–6061.
[18] J. R. Long, O. M. Yaghi, *Chem. Soc. Rev.* **2009**, *38*, 1213–1214.
[19] H. B. Tanh Jeazet, C. Staudt, C. Janiak, *Dalton Trans.* **2012**, *41*, 14003–14027.
[20] S. R. Batten, N. R. Champness, X.-M. Chen, J. Garcia-Martinez, S. Kitagawa, L. Öhrström, M. O'Keeffe, M. P. Suh, J. Reedijk, *CrystEngComm* **2012**, *14*, 3001–3004.
[21] T. Stolar, K. Užarević, *CrystEngComm.* **2020**, *22*, 4511–4525.
[22] R. I. Walton, *Chem. Soc. Rev.* **2002**, *31*, 230–238.
[23] J. Heine, T. Wehner, R. Bertermann, A. Steffen, K. Müller-Buschbaum, *Inorg. Chem.* **2014**, *53*, 7197–7203.
[24] Z. Wang, S. M. Cohen, *Chem. Soc. Rev.* **2009**, *38*, 1315–1329.
[25] Z. Wang, K. K. Tanabe, S. M. Cohen, *Inorg. Chem.* **2009**, *48*, 296–306.
[26] N. Y. Gugin, A. Virovets, E. Peresypkina, E. I. Davydova, A. Y. Timoshkin, *CrystEngComm.* **2020**, *22*, 4531–4543.
[27] J. Heine, M. Hołyńska, M. Reuter, B. Haas, S. Chatterjee, M. Koch, K. I. Gries, K. Volz, S. Dehnen, *Cryst. Growth Des.* **2013**, *13*, 1252–1259.
[28] T. Schäfer, K. Müller-Buschbaum, *Z. Anorg. Allg. Chem.* **2018**, *644*, 1791–1795.
[29] T. Schäfer, A. E. Sedykh, J. Becker, K. Müller-Buschbaum, *Z. Anorg. Allg. Chem.* **2020**, *646*, 1555–1562.
[30] M. E. Schweinefuß, I. A. Baburin, C. A. Schröder, C. Näther, S. Leoni, M. Wiebcke, *Cryst. Growth Des.* **2014**, *14*, 4664–4673.
[31] T. N. Sevastianova, E. I. Davydova, I. V. Kazakov, A. Y. Timoshkin, *Russ. Chem. Bull.* **2015**, *64*, 2523–2535.
[32] T. N. Sevastianova, M. Bodensteiner, A. F. Maulieva, E. I. Davydova, A. V. Virovets, E. V. Peresypkina, G. Balázs, C. Graßl, M. Seidl, M. Scheer, G. Frenking, E. A. Berezovskaya, I. V. Kazakov, O. V. Khoroshilova, A. Y. Timoshkin, *Dalton Trans.* **2015**, *44*, 20648–20658.
[33] A. Zurawski, F. Hintze, K. Müller-Buschbaum, *Z. Anorg. Allg. Chem.* **2010**, *636*, 1333–1338.
[34] J. Heine, M. Hołyńska, M. Reuter, B. Haas, S. Chatterjee, M. Koch, K. I. Gries, K. Volz, S. Dehnen, *Cryst. Growth Des.* **2013**, *13*, 1252–1259.
[35] S. P. Petrosyants, *Russ. J. Inorg. Chem.* **2013**, *58*, 1605–1624.
[36] S. P. Petrosyants, A. B. Ilyukhin, *Russ. J. Inorg. Chem.* **2010**, *55*, 30–33.
[37] S. P. Petrosyants, A. B. Ilyukhin, *Russ. J. Inorg. Chem.* **2011**, *56*, 2047–2069.
[38] C. R. Samanamú, A. F. Richards, *Polyhedron* **2007**, *26*, 923–928.
[39] T. N. Sevastianova, M. Bodensteiner, A. S. Lisovenko, E. I. Davydova, M. Scheer, T. V. Susliakova, I. S. Krasnova, A. Y. Timoshkin, *Dalton Trans.* **2013**, *42*, 11589–11599.
[40] R. G. Pearson, *Inorg. Chim. Acta* **1995**, *240*, 93–98.
[41] M. O'Keeffe, M. A. Peskov, S. J. Ramsden, O. M. Yaghi, *Acc. Chem. Res.* **2008**, *41*, 1782–1789.
[42] S. Natarajan, P. Mahata, *Chem. Soc. Rev.* **2009**, *38*, 2304–2318.
[43] A. F. Wells, *Three Dimensional Nets and Polyhedra*, Wiley **1977**.
[44] H. Furukawa, Y. B. Go, N. Ko, Y. K. Park, F. J. Uribe-Romo, J. Kim, M. O'Keeffe, O. M. Yaghi, *Inorg. Chem.* **2011**, *50*, 9147–9152.
[45] J. A. J. Pardoe, A. R. Cowley, A. J. Downs, T. M. Greene, *Acta Crystallogr. Sect. C* **2005**, *61*, m200-m202.
[46] N. M. Boag, K. M. Coward, A. C. Jones, M. E. Pemble, J. R. Thompson, *Acta Crystallogr. Sect. C* **1999**, *55*, 672–674.
[47] S. Ide, N. Karacan, Y. Tufan, *Acta Crystallogr. Sect. C* **1995**, *51*, 2304–2305.
[48] J. D. Forrester, A. Zalkin, D. H. Templeton, *Inorg. Chem.* **1964**, *3*, 63–67.
[49] G. Sheldrick, *Acta Crystallogr. Sect. C* **2015**, *71*, 3–8.
[50] G. Sheldrick, *Acta Crystallogr. Sect. A* **2015**, *71*, 3–8.
[51] O. V. Dolomanov, L. J. Bourhis, R. J. Gildea, J. A. K. Howard, H. Puschmann, *J. Appl. Crystallogr.* **2009**, *42*, 339–341.
[52] W. Pennington, *J. Appl. Crystallogr.* **1999**, *32*, 1028–1029.
[53] V. A. Blatov, A. P. Shevchenko, D. M. Proserpio, *Cryst. Growth Des.* **2014**, *14*, 3576–3586.

Manuscript received: February 12, 2021
Revised manuscript received: March 30, 2021
Accepted manuscript online: April 12, 2021

